Cleaner Food Systems 3 (2026) 100031

Contents lists available at ScienceDirect

Cleaner Food Systems

journal homepage: www.sciencedirect.com/journal/cleaner-food-systems

Restoration potential of degraded landscapes for strengthening rural livelihoods

Venkata Radha Akuraju, Kaushal K. Garg, K.H. Anantha *, Shishuvendra Kumar, Ashok Shukla, Ramesh Singh, Bhabani Sankar Das, M.L. Jat

International Crops Research Institute for the Semi-Arid Tropics (ICRISAT), India

ARTICLE INFO

Keywords:
Multifunctional landscape
Ecosystem services
Groundwater resilience
Water scarcity
Water budget

ABSTRACT

Land degradation in rainfed semi-arid regions is driven by deforestation, soil erosion, and water scarcity posing a major threat to agricultural production and rural livelihood. Declining moisture retention capacity in these areas are reducing soil moisture storage and limiting groundwater recharge leading to higher dependency on supplemental irrigation and ultimately constraining cropping intensity and farm income. Recognising these challenges, we examined an integrated set of landscape resource conservation interventions and assessed the restoration potential of degraded ecologies using Bundelkhand region of Central India as an example. Accordingly, rainwater harvesting measures were deployed across a 255-ha watershed between 2018 and 2022. An innovative range of engineering structures were designed and implemented to harvest runoff water at foothills along with various in-situ interventions in adjoining agricultural fields. Continuous hydrologic and socio-economic monitoring were undertaken to evaluate the impacts of these interventions on water resources, cropping intensity, and household incomes. Improved water retention and infiltration regime enabled the harvesting of about 210 mm of runoff water in upland areas, which translated to 105-180 mm of additional groundwater recharge at a cluster scale. As a result, groundwater levels rose by 4-6 m, enabling reliable irrigation during *rabi* season (Nov - Mar) compared to the non-intervention (baseline) conditions. Changes in both soil moisture and groundwater regimes led to the increase in the cultivated area from 4 ha in 2018 to over 100 ha by 2021. In fact, previously fallow lands were brought under double cropping being supported by enhanced recharge and shallow aquifer availability. With cropping intensification and improved yield stability, total annual net income at the cluster scale increased from USD 2370 to USD 148,500. This corresponded to an increase in average annual household income from USD 52 in 2019 to USD 3300 in 2023. Furthermore, a notable outcome of this initiative was that 45 previously migrated families returned back to their home and resumed farming. Thus, spatially-explicit landscape restoration such as decentralized rainwater harvesting through proper hydrologic planning and community participation can effectively reverse land degradation. Such a model offers a replicable framework for scaling sustainable land and water management practices across similar degraded landscapes of Asia, Africa and beyond, contributing meaningfully to climate adaptation, food security, and the Sustainable Development Goals.

1. Introduction

Land degradation is one of the most pervasive environmental and socio-economic challenges worldwide affecting nearly 29% of the Earth's terrestrial land surface and about 3.2 billion people (Feng et al. 2025). Land degradation includes soil erosion, nutrient depletion, desertification, biodiversity loss, and the depletion and contamination of water resources among others (IPBES, 2018; Olsson et al. 2019; Deng et al. 2025). These processes undermine ecosystem functioning and directly impair key ecosystem services such as freshwater availability, agricultural productivity, carbon sequestration and climate regulations (Montanarella et al. 2016; Xie et al. 2020; Wiebe and Wilcove, 2025). The consequences of land degradation are particularly severe for rural populations, especially in developing countries where livelihood heavily

* Corresponding author. Regenerative Landscape Theme, Global Research Program – Resilient Farming Systems, International Crops Research Institute for the Semi-Arid Tropics (ICRISAT), Patancheru, 502324, Telangana, India.
E-mail address: Anantha.kanugod@icrisat.org (K.H. Anantha).

https://doi.org/10.1016/j.clfs.2026.100031
Received 12 February 2026; Received in revised form 2 March 2026; Accepted 26 March 2026
Available online 27 March 2026

depends on agriculture and on land and water resources (Garg et al 2020a, 2022; Singh et al 2021, 2022).

Land degradation is driven largely by land use change associated with population growth, economic development, and expanding agricultural frontiers (Garg et al. 2020b). For example, deforestation has become a major concern in upland areas, where forests serve as critical source of baseflow and biodiversity (Rockstrom et al. 2009; Gleeson et al. 2012; Famiglietti, 2014; de Graaf et al. 2019). Baseflow is the sustained portion of river flow supplied by groundwater, which maintains perenniality of river flow and spring discharge (Frisbee et al., 2022). The removal of vegetation cover disrupts the natural hydrologic cycle by reducing soil infiltration, intensifying surface runoff, and accelerating the sediment transport to downstream ecosystems (Ellison et al. 2017; Gashaw et al. 2018). These processes contribute to flooding, siltation of rivers and reservoirs, eutrophication of freshwater bodies, and declining water quality (Sun et al. 2018; Vogt et al. 2021; Sharma et al., 2024). Climate change further amplifies these pressures by altering rainfall patterns and increasing the frequency of extreme events, while biodiversity losses reduce ecosystem resilience and recovery capacity (Gleeson et al. 2012; Richardson et al. 2023). Together, these interacting stresses create reinforcing feedbacks that accelerate environmental degradation and threaten the sustainability of both nature and human systems (Leal Filho et al. 2019).

Agricultural systems, particularly those that are rainfed, are among the most vulnerable ones to land degradation (Barbier and Hochard, 2018). Rainfed agriculture accounts for more than 80% of global cultivated land and supports the livelihoods of hundreds of millions of smallholder farmers, many of whom operate in fragile and marginal environments (FAO, 2019; Lipper et al. 2017). Heavily reliant on seasonal rainfall, these systems lack access to irrigation infrastructure and are, often, characterized by poor soil fertility and limited access to inputs (Anantha et al 2021a, 2021b). As land degradation intensifies, rainfed systems face declining water availability, reduced soil productivity, and greater susceptibility to crop failure (Dinar et al., 2019; Fitton et al. 2019). This has direct implications for food security, income stability, and nutrition, particularly in regions already experiencing high levels of poverty and malnourishment such as Asia and Africa (Ferrant et al. 2014; MacDonald et al. 2016; Anantha et al. 2022).

Combined pressures of land degradation and water scarcity have rendered large areas of agricultural land either seasonally or permanently fallow (Plassin et al. 2021; Pal et al. 2023). This has forced communities to seek new land for cultivation, often by clearing forests and converting other ecologically sensitive areas into farmland (Nkonya et al. 2016). While such land use changes may offer short-term gains in agricultural output, they often come at the cost of long-term sustainability, leading to further environmental degradation and a decline in ecosystem resilience (Plassin et al. 2021). Although substantial research has been devoted to studying the impacts of land use change, particularly deforestation and agricultural expansion, on hydrology, nutrient cycling, and crop productivity, there is a notable lack of experimental evidence on how degraded landscapes can be effectively restored. In particular, the impacts of landscape restoration on water regulation, biodiversity enhancement, ecosystem service recovery, and the socio-economic conditions of smallholder farmers remain underexplored (Sayer et al. 2013; Reed et al. 2020; Anantha et al 2021c; Mansour et al. 2022; Khosravi Mashizi and Sharafatmandrad, 2025). Moreover, existing hydrologic and environmental studies tend to focus on large-scale catchment or river basin scales, making their findings difficult to translate into localized and actionable interventions (van Griensven et al. 2016). The scale mismatch between scientific research and real-world application has hindered the effective implementation of sustainable land and water management practices. Restoration efforts must, therefore, be adapted to smaller spatial units such as individual landholdings (ranging from 1 to 10 ha) and meso-scale watersheds (from 10 to 5000 ha) where resource management decisions are made and implemented (Keesstra et al. 2018). At these scales, context-specific strategies are to be designed, which aligns well with local agroecological conditions, land-use patterns, and water needs of different cropping systems.

In response to the urgent need for sustainable land management, the overall objective of this study is to evaluate the interconnected impacts of landscape restoration on hydrologic processes, ecosystem services, and smallholder livelihoods with a major goal to identify key spatially-explicit and data-driven strategies that are responsive to local environmental and socio-economic contexts, and are capable of generating co-benefits for both ecosystems and rural communities. Thus, the specific objectives of the study are to i) assess the effects of land restoration on hydrological dynamics, including improvements in water retention, reduced surface runoff, and overall watershed functioning; ii) evaluate the influence of land restoration on agricultural production, with particular attention to crop intensification, yield stability, and farming system productivity in rainfed areas; and iii) examine the socio-economic outcomes for smallholder communities, such as enhanced rural livelihoods, income generation, and food security.

2. Materials and methods

2.1. Study area

The Bundelkhand region of the Central Indian Landscape is one of the hotspots of poverty, malnutrition, land degradation, poor agriculture, and low livestock productivity (Singh et al 2014, 2022; Sahu et al. 2015; Garg et al. 2020a). The region spans across 6.9 million ha between the states of Madhya Pradesh and Uttar Pradesh, comprising 14 districts and a population of 15.5 million (NITI Aayog, 2016). This region receives 700-1000 mm of annual rainfall, yet suffers from water scarcity and land degradation because of poor groundwater recharge (Singh et al 2019, 2022). With its characteristic hard-rock geology, groundwater recharge in this region primarily occurs in shallow and unconfined aquifers, which are characterized by poor specific yield (0.5-5.0%). The water levels in dug wells (4-8 m deep) deplete rapidly after the rainy season, leaving communities to endure water scarcity, especially during the post-rainy months (Singh et al 2014, 2021; Garg et al. 2020a).

The region is characterized by undulating topography, high temperatures, erratic rainfall, and low soil fertility contributed to poor agricultural productivity (0.5-2.0 t ha^{-1}) and food insecurity (Shakeel et al. 2012; Padhan et al. 2025). Farmers in the region grow water-efficient crops, such as groundnut, black gram, sesame, and millets during the *kharif* season, and wheat, chickpea, barley, mustard, and lentils during the *rabi* season (Padhan et al. 2025). Crops grown during the *kharif* season may require supplemental irrigation during dry spells, while most crops grown in the *rabi* season rely on irrigation support. The region has a high incidence of poverty (30-55% in different districts), a low literacy rate (57% overall, 43% for women), and a highly vulnerable population of women and landless people (Varua et al. 2018; Mitra and Rao, 2019; Padhan et al. 2025).

With support from the Government of Uttar Pradesh, the International Crops Research Institute for the Semi-Arid Tropics (ICRISAT) carried out a research-for-development initiative in the Bundelkhand region between 2018 and 2022. As a part of this initiative, the Poora Birdha (Lat/Long: 25.12008N, 78.53769E) village was selected as a target site for restoring its degraded lands. Poora Birdha is located in the uppermost part of the landscape and is characterized by undulating topography and multi-directional slopes. The uplands of the village are degraded barren hillocks, which generating large quantities of runoff water that floods the agricultural land situated at the foothills making it difficult to practice agriculture during the *kharif* season and leading to severe water scarcity in the *rabi* season. The area is dominated by Alfisols, and farmers in the area cultivate groundnut, black gram, sesame, and millets during the *kharif* period, and wheat, mustard, chickpea and field pea in the *rabi* season. The village has an agricultural area of 121 ha with a hydrologic catchment area of 255 ha. Although 55 farming

families inhabit this village, water scarcity had forced many farmers to abandon agriculture and migrate to nearby urban centres in search of livelihood. By 2018, only four families were residing in the village.

2.2. Landscape resource conservation interventions

Before implementing landscape resource conservation interventions, topography survey and soil profiling were conducted for identifying a range of *in-situ* and *ex-situ* rainwater harvesting interventions. After detailed hydrologic analyses, five rainwater harvesting structures with masonry core wall and outlets at suitable location at foothills were constructed (Figs. 1 and 2). Besides, large fields were divided into 0.4-0.8 ha of plots with earthen field bunding along with field drainage structure to dispose-off excess runoff, so as to prevent breaching of the field bunds during heavy downpours. These earthen bunds were strengthened by introducing teak based agroforestry system. To control flooding in agricultural fields and safely dispose-off excess runoff, diversion drains were excavated across the landscape covering 3000 running meters. Generated runoff from the barren hillocks was first harvested into masonry structures whereas those from agriculture fields was harvested in the form of soil moisture by intensive field bunding and excavation of farm ponds. Altogether, 150,000 cubic meter storage capacity was created which was measured by topography survey using a differential geographical position system (DGPS). In this approach, both masonry and earthen works were integrated to optimise the cost and sustainability of the structures. Fig. 1 shows the location of large-scale masonry structures, field drainage structures, farm ponds, field bunding and diversion drains.

2.3. Data monitoring and analysis

2.3.1. Soil biophysical and nutrient characterization

Surface soil samples (0-15 cm depth) were systematically collected from each 10 ha grid across the study area to evaluate key soil biophysical and nutrient properties. Collected samples were air-dried, grinded, and sieved through a 2 mm mesh sieve for laboratory analysis. Soil texture was determined using the hydrometer method. Soil organic carbon (SOC) content was estimated using the Walkley and Black wet oxidation method. Soil water retention characteristics such as the water contents at field capacity (FC) and permanent wilting point (PWP) were measured using a pressure plate apparatus. Soil nutrient analysis was undertaken, which included available phosphorus (Av. P) using the Olsen's method and available potassium (Av. K) through flame photometry method. Selected micronutrients such as zinc (Zn), iron (Fe), manganese (Mn), and copper (Cu) were analysed using the DTPA (diethylenetriaminepentaacetic acid) extraction followed by Atomic Absorption Spectrophotometry (AAS).

2.3.2. Hydrologic monitoring

Hydrologic data were collected from both field and reservoir outlets to quantify runoff generation and groundwater recharge at daily, monthly and seasonal time scales. Water balance was evaluated with a specific focus on surface runoff and groundwater recharge, which are the primary components that govern hydrologic responses (Garg et al. 2020a). Major water balance equation is defined by Eq. 1

$$Rainfall\ (mm) = Surface\ runoff\ (mm) + Groundwater\ recharge\ (mm) + \Delta S\ (mm) \quad \text{Eq.1}$$

where ΔS represents the residual storage change. Because soil moisture dynamics and evapotranspiration were not measured independently, these were not explicitly included in the water balance equation and are treated as residual components.

i) Reservoir hydrology

An automatic rain gauge was used to record rainfall data on hourly time scale. Runoff gauging stations were established at selected outlets of rainwater harvesting structures built during the landscape resource conservation initiative indicated by S1, S2, S4, S5 in Fig. 1. A detailed description of runoff gauging station can be referred from Garg et al. (2020a). Runoff gauging stations were placed at masonry structures

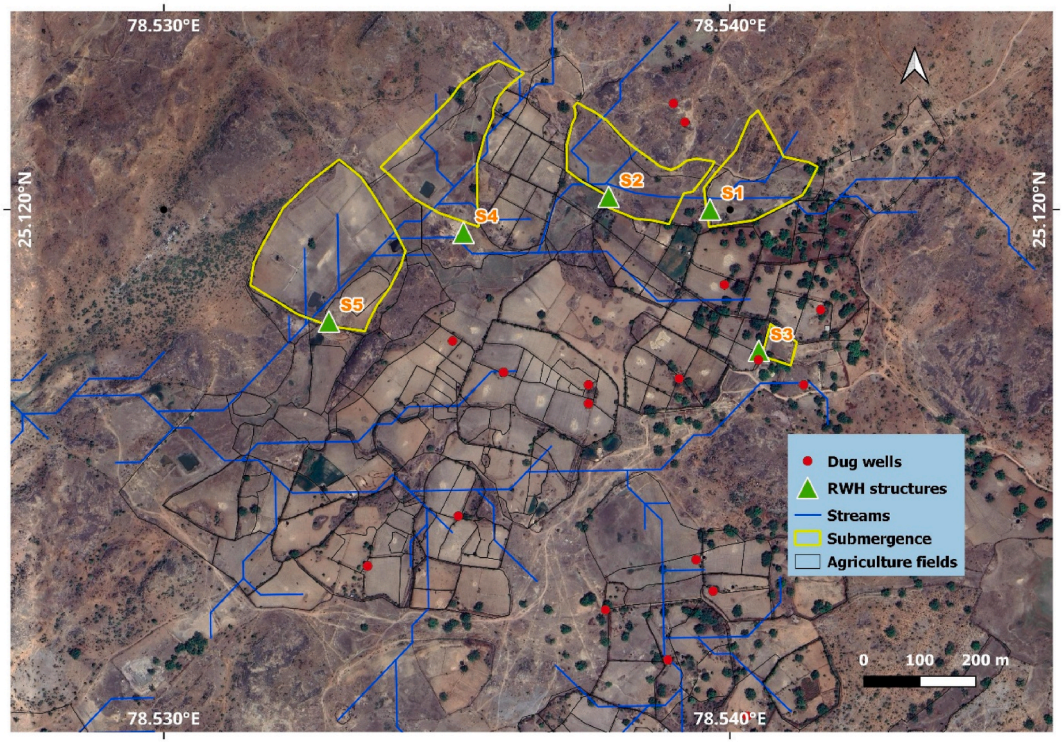

Fig. 1. Location of Poora-Birdha village, Lalitpur district, Uttar Pradesh.

Fig. 2. Selected images of landscape resource conservation interventions, runoff monitoring stations, groundwater well, and cultivated crops in the study area; Panel 1 (left): Drone view of the study area showing constructed water bodies at the foothills, diversion drains, and field bunding; Panel 1 (right): Zoomed-in view of the first rainwater-harvesting structure constructed at the foothill; Panel 2 (left and right): Zoomed-in views of field bunds with masonry surplus structures; Panel 3 (left and right): Hydrologic monitoring systems at field (S3) and reservoir outlet (S1); Panel 4 (left): Dug well with elevated water table in October 2022; Panel 4 (right): Aerial view of the study area with crops during the rabi season in 2022.

(refer Fig. 2) in which a DIVER (Digital In Situ Versatile Environmental Recorder, i.e., pressure transducers, Van Essen Instruments, The Netherlands) was used to measure water heads to estimate the changes in reservoir storage and outflow volumes. Following two equations were used to estimate inflow and outflow volumes at each reservoir based on continuous water-level measurements recorded by the DIVER:

$$\sum_{i=1}^{n} \text{Inflow}_i = \sum_{i=1}^{n} \Delta RS_i + \sum_{i=1}^{n} \text{Outflow}_i \quad \text{Eq. 2}$$

$$\text{Outflow}_i = \int_{t_{i-1}}^{t_i} 1.71 L H^{3/2}\, dt \quad \text{Eq. 3}$$

where inflow and outflow were expressed in m^3 sec^{-1}, L is the crest length of the structure (m), and H is the amount of the spillover overhead measured (in meter) by DIVER pressure transducer at respective runoff events. In Eqs. (2) and (3), i and t denote discrete time steps during a runoff or spillover event (*i.e.*, 15 min in current study), n is the total number of time intervals considered for each event and ΔRS_i is the

change in reservoir storage (m^3) during time step *i*.

Stage-volume relationships of the respective reservoirs were developed for each reservoir by undertaking detailed DGPS-based topography surveys, allowing reservoir storage to be estimated at 1 cm water level increments. Changes in reservoir volume between two successive time steps (ΔV) were used to infer hydrologic fluxes. A positive ΔV indicates net runoff inflow to the reservoir, ΔV = 0 indicates a balance between inflow and percolation contributing to groundwater recharge. The runoff volume measured for each event (m^3) was converted into an equivalent water depth (mm) using the contributing catchment area.

The number of times each structure was filled was estimated by comparing cumulative inflow volumes with the effective storage capacity derived from the stage–volume relationship. Continuous DIVER pressure transducer-based measurements of inflow, spillover, and changes in reservoir storage were used to calculate the total volume of water entering each reservoir during a season. The net retained volume, calculated as cumulative inflow minus cumulative spillover, was divided by the reservoir's storage capacity to estimate how many times the structure was effectively filled and emptied during the rainy season.

ii) Runoff from agricultural field

The V-notch weir provides high sensitivity for measuring low to moderate runoff flows, making it particularly suitable for small agricultural catchments (Rantz, 1982). The sharp-crested triangular notch allows accurate estimation of discharge over a wide range of flow conditions. Runoff from the 2.8 ha agricultural catchment was measured using a 45° V-notch weir equipped with a DIVER pressure transducer (refer S3 in Fig. 1; Panel 3 in Fig. 2). Runoff volume for each event was calculated by integrating discharge (Q) over time as shown in Eq. (4):

$$Runoff = \sum_{i=1}^{n} Q_i \times \Delta t, \quad \text{Eq. 4}$$

where Q_i represents the runoff discharge ($m^3\ s^{-1}$) at time step *i*, and H_i is the water head (m) above the crest of the V-notch measured by the DIVER at the same time step. The runoff volume measured for each event (m^3) was converted into an equivalent water depth (mm) using the contributing catchment area.

iii) Groundwater recharge and its use

Groundwater is the primary source of freshwater for both domestic and agricultural uses in the studied watershed with dug wells distributed across the agricultural landscape (indicated by red dots in Fig. 1). Groundwater levels were monitored in 18 representative dug wells on a monthly basis from 2019 onward using manual water-level indicators. Water-level indicators is a standard electric tool, which emit an audible and visual signal upon contact with the water surface, allowing accurate determination of depth to groundwater from a fixed reference point. Water level measurements were taken from the same reference mark in each well to ensure consistency and comparability over time. These measurements were used to quantify seasonal groundwater table fluctuations across the study area.

Using water table data, groundwater recharge, its utilization and available storage in shallow aquifer were estimated using the water table fluctuation (WTF) method, a widely applied approach in hard-rock aquifers (Sharda et al. 2006; Dewandel et al. 2010; Glendenning and Vervoort, 2010; Garg et al. 2020b). Net groundwater recharge was calculated using Eq. (5):

$$R_i = \Delta h_i \times S_y \times 10 + W_i \quad \text{Eq. 5}$$

where R_i is net groundwater recharge (mm) during the *i*th time period, Δh is the change in hydraulic head (m) between time intervals of groundwater levels, and S_y is the specific yield of the aquifer (dimension less), and W_i is the groundwater withdrawal (mm) by pumping during the same period. A specific yield (S_y) of 0.03 was adopted based on earlier studies in this hard-rock aquifer system (Singh et al. 2014; Garg et al. 2020b).

To quantify groundwater pumping pattern for the major cropping systems, DIVERs were installed in five representative dug wells and programmed to record hydraulic head at 10 min intervals. Pump operation causes an abrupt drawdown in groundwater level, which is captured by the high-frequency monitoring. A drop in hydraulic head greater than 10 mm (0.01 m) within a 10 min interval was used as an operational threshold to identify active pumping periods. Pumping duration was computed by summing all time intervals during which this threshold was exceeded, thereby providing an objective and observation-based estimate of pumping hours. In addition, pump capacity and energy consumption, along with the area cultivated, crop yield, and total production for different crops were recorded for five representative farm fields during both the *kharif* and *rabi* seasons. The volume of water pumped was estimated using Eq. (6):

$$Q = \frac{P\ x\ Pump\ Efficiency}{H\ x\ g\ x\ \rho} \quad \text{Eq. 6}$$

where Q is the pump discharge ($m^3\ sec^{-1}$), P is the pump power (Watt), g is the acceleration due to gravity (=9.8 $m\ s^{-2}$), ρ is the density of water (=1000 $kg\ m^{-3}$), and H is the total head (m). We assumed a pump efficiency of 85% in our study. Additionally, a 3-m head loss was incorporated into the total head value following Singh et al. (2021) to account for head losses because of pipe joints and system friction. Total irrigation volume was then calculated using Eq. (7):

$$\text{Irrigation volume } (m^3) = Q\ (m^3\ sec^{-1}) x\ t\ (\text{hours of pumping}) \times 3600\ (sec\ hour^{-1}) \quad \text{Eq. 7}$$

2.3.3. Crop intensification, crop yield and net income

An intensive ground data collection campaign was undertaken to assess the impact of landscape resource conservation on crop intensification, crop yield and net income. Total 121 ha of cultivable agricultural land from the study cluster was divided into 185 field parcels based on their boundary demarcation. Entire agricultural field parcels were delineated and crop cultivated during *kharif* and *rabi* seasons were recorded in each of these parcels between 2018 and 2023. Further, normalized difference vegetation index (NDVI) analysis was undertaken to understand the year-wise change in cropping intensity, which was further verified by ground survey. NDVI <0.2 indicates no vegetation; NDVI = 0.2–0.4 sparse vegetation; NDVI = 0.4–0.6 moderately dense vegetation; and NDVI >0.6 dense vegetation (Elsu et al., 2017). In this study, NDVI values greater than 0.4 were used as an indicative threshold for cropped fields and seasonal crop cover, and these classifications were systematically validated through field-parcel–level ground surveys conducted during both kharif and rabi seasons.

Out of total 210 field parcels, 20 fields with 0.4-1.0 ha size (belongs to 10 farmers) were chosen for intensive monitoring of crop yield, cost of cultivation and net income. For crop yield measurements, crop cutting studies were undertaken by demarcating a 5 m × 5 m area from respective monitoring fields. Harvested crop after the maturity from the demarcated area was air-dried and grain weight was measured. These values were converted in terms of crop yield per ha in respective seasons (*kharif* and *rabi*).

To estimate the net income generated from agriculture, data on cost of cultivation were recorded which includes tillage operation, seed and fertilizer cost, energy cost for irrigation, labour involved in sowing, irrigation application, interculture operations and crop harvesting. Minimum support price of different crops for respective years was taken from the Directorate of Economics and Statistics, Ministry of Agriculture and Farmers Welfare, Government of India (Government of India, 2024) and net income was calculated using Eq (8):

$$\text{Net income } (₹) = \text{Crop yield } (₹) \times \text{Market price } (₹) - \text{Cost of cultivation } (₹) \quad \text{Eq. 8}$$

Further livestock income was calculated by adding income from milk (after deducting the management cost).

2.3.4. Household level socio-economic assessment

A household survey was conducted through face-to-face interviews between March and July 2023. All 45 households were surveyed for understanding the impact of landscape resource conservation measures on household income and migration status. Data collection was carried out by trained enumerators who were fluent in the local language and well-acquainted with the region. The questionnaire was translated into local language to eliminate any misunderstanding during the data collection. The questionnaire gathered detailed information on household demographics, primary occupations, livelihood strategies, time management for domestic and agricultural operations, farm resources, crop and livestock patterns before (2017) and after project interventions (2018-2022). Resource availability status in terms of groundwater availability and their interest in practicing agriculture were analysed. Migration and wage employment status were also recorded for all households.

2.3.5. Statistical analysis

Statistical analyses were performed to assess changes in hydrological, agricultural, and socio-economic indicators following the implementation of landscape resource conservation interventions. Net groundwater availability, crop yields, and total agricultural income were analysed using one-way Analysis of Variance (ANOVA) by comparing pre-intervention (2019) and post-intervention (2020–2023) periods. Monthly well-level groundwater availability was evaluated by classifying dug wells into three categories based on hydraulic head: dry, 1–3 m, and >3 m. Changes in the distribution of wells across these categories before and after interventions were tested using a Chi-square test. Agricultural income data were derived from annual household surveys and aggregated at the landscape scale. Net income from kharif and rabi crops, livestock, and total annual income were analysed using one-way ANOVA to assess intervention effects.

3. Results

3.1. Rainfall-runoff relationship and reservoir hydrology

The soils of the study area are predominantly coarse textured, with high sand (coarse sand: 51.7% and fine sand: 25.9%) and low clay contents (9.9%) (Table 1). Silt content averaged at 12.5% indicating a generally light-textured, highly permeable soil profile. The soils were slightly acidic to neutral (pH: 6.66) with low electrical conductivity (0.20 dS m^{-1}), suggesting non-saline conditions suitable for crop growth. However, SOC content was low to moderate (average SOC: 0.66%) indicating limited water- and nutrient-holding capacity for the studied soils.

Table 1
Soil physical and nutrient parameters measured at study site.

Parameters	Unit	Values
Coarse sand	%	51.7 (12)
Fine sand	%	25.9 (9)
Silt	%	12.54 (5)
Clay	%	9.86 (7)
pH	-	6.66 (10)
Electrical Conductivity	(dS/m)	0.20 (104)
Organic Carbon	Per cent	0.66 (41)
Available P	mg/kg	24.4 (63)
Exchangeable K	mg/kg	77 (129)
Exchangeable. Ca	mg/kg	1150 (56)
Exchangeable. Mg	mg/kg	206 (47)
Available. S	mg/kg	10.7 (108)
Available Zn	mg/kg	1.21 (7.3)
Available B	mg/kg	0.43 (60)
Available Fe	mg/kg	20.6 (99)
Available Cu	mg/kg	0.75 (85)
Available Mn	mg/kg	21.7 (55)
Available Na	mg/kg	67.3 (43)

No of samples analysed: 176.

Fig. 3 illustrates the daily rainfall distribution of 2021-22 and corresponding water storage levels in S1. During June, rainfall events were relatively low to moderate in intensity, with daily values generally not exceeding 40 mm. The cumulative rainfall during this period reached approximately 200 mm. However, this amount was insufficient to generate any inflow into the reservoir, because the existing dry soil conditions and weathered zone of the hillock absorbed most of the initial rainfall. A major rainfall event occurred on July 25, 2021 with 140 mm of rainfall. This high-intensity storm generated substantial runoff resulting in significant inflow to the reservoir and rapidly filling it to its full storage capacity of 22,000 m^3. Any additional runoff beyond this capacity was released as spill-over. Following this event, the harvested water in the reservoir began to infiltrate gradually, with an infiltration rate of approximately 18-22 mm day^{-1}, reflecting natural seepage into the subsurface. During September and October, intermittent rainfall events continued to generate inflows, repeatedly restoring the reservoir to its full capacity and storage remained at or near-full level for extended period in September.

Towards the last week of October, rainfall started to reduce causing inflow to cease and the reservoir storage began to steadily decline. The depletion occurred at an average rate of 15-20 mm day^{-1}, primarily because of infiltration and minor evaporation losses. Notably, the infiltration rate observed in August was comparable to that during October–November indicating that the infiltration capacity of the same reservoir remained stable even after several months of water storage. This sustained infiltration is attributed to the reservoir's location at the foothills, i.e., in the uppermost part of the landscape and also light textured soils, where a relatively high hydraulic gradient promoted continuous downward movement of water into subsurface zone. Thus, the natural topographic setting facilitated persistent recharge throughout the rainy season.

Fig. 4 illustrates the cumulative inflow and outflow (spill-over) measured at S1 in relation to the cumulative rainfall received during the year 2021–22. The catchment of S1 is 34 ha and consists largely of a degraded hillock with 5-7% slope. Consistent with early-season soil wetting phase described above, inflow into the structure began only after approximately 200 mm of cumulative rainfall had been received. The total annual rainfall recorded during 2021–22 was 950 mm, of which 55% was converted into runoff. The total volume of water that spilled over from S1 was equivalent to 320 mm of the contributing catchments, which corresponds to about 34% of the total rainfall received. The difference between cumulative inflow and spill-over (i.e., 210 mm) represents the volume of water effectively harvested and stored in the structure. Spill-over was first recorded only after the cumulative rainfall reached about 400 mm indicating that the initial runoff was retained within the structure up to that point. Further, Fig. 5 depicts the number of times the S1 filled during 2021-22. Given its storage capacity of 22000 m^3, the structure was filled once after 400 mm of cumulative rainfall; twice after 800 mm, and three times after 900 mm of rainfall. Overall, the reservoir was filled 3.2 times during the year, demonstrating its effectiveness in capturing and storing runoff from the contributing catchment.

3.2. Comparison of runoff generation from different land uses

Fig. 6 shows a comparative analysis of runoff generated from two distinct land use types of degraded hillock and agricultural land. The degraded hillock has a 5-7% slope and shallow soils (<15 cm) with about 30% surface covered by exposed rocks. In contrast, the

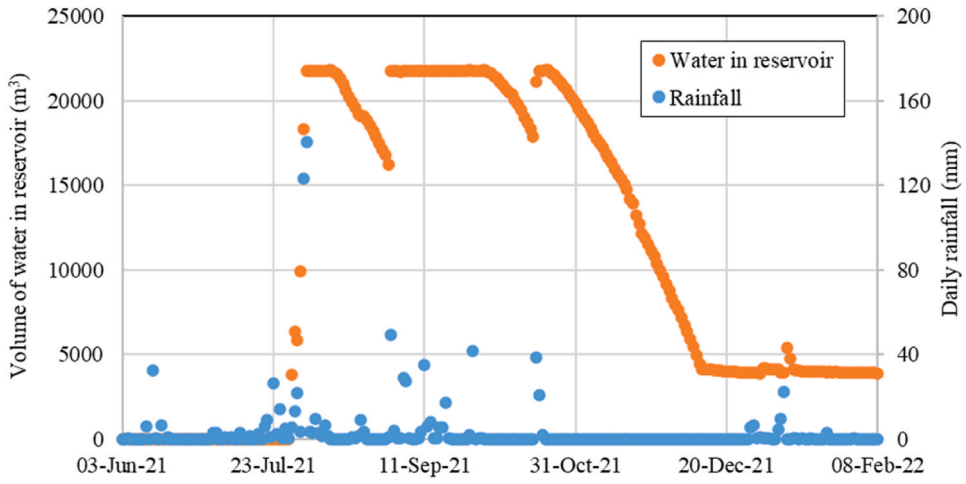

Fig. 3. Distribution of rainfall and stored water in reservoir during 2021-22 at S1.

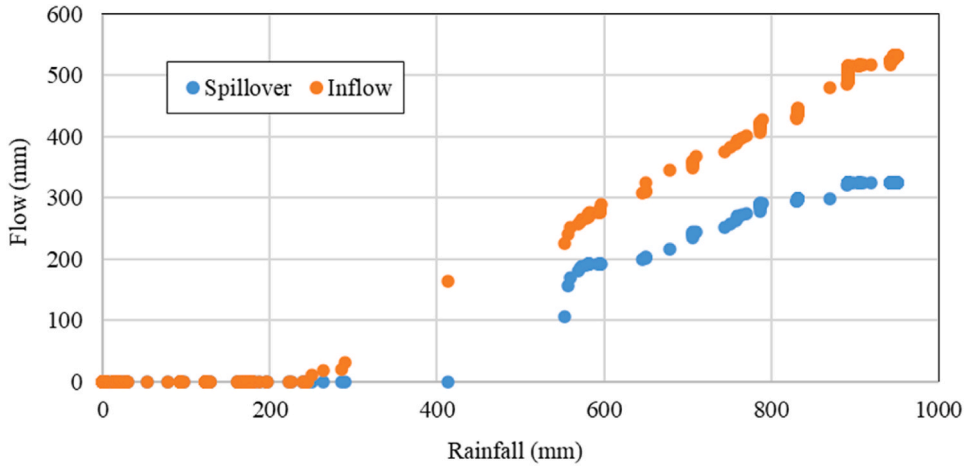

Fig. 4. Inflow and spillover amount measured against cumulative rainfall received during 2021-22 at S1.

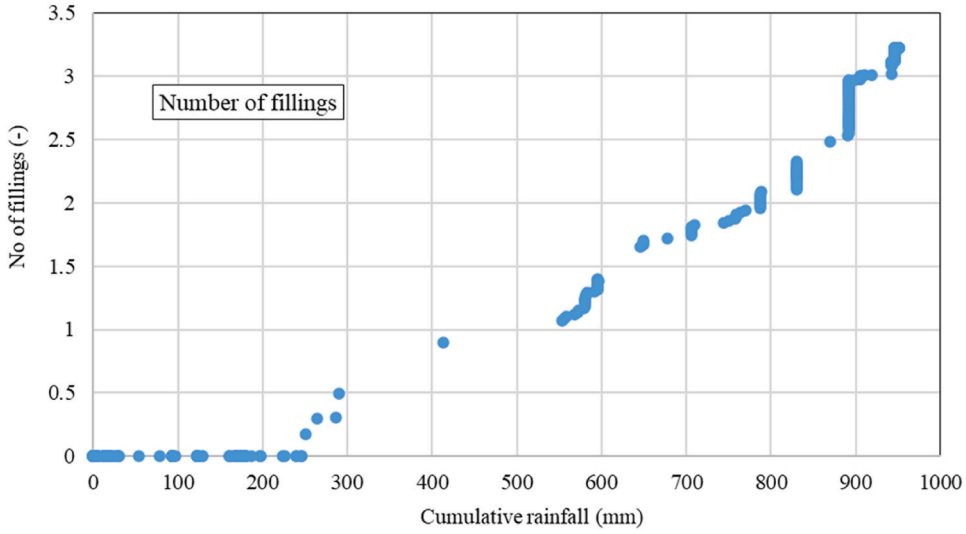

Fig. 5. Number of fillings measured corresponding to cumulative rainfall received during 2021-22 at S1.

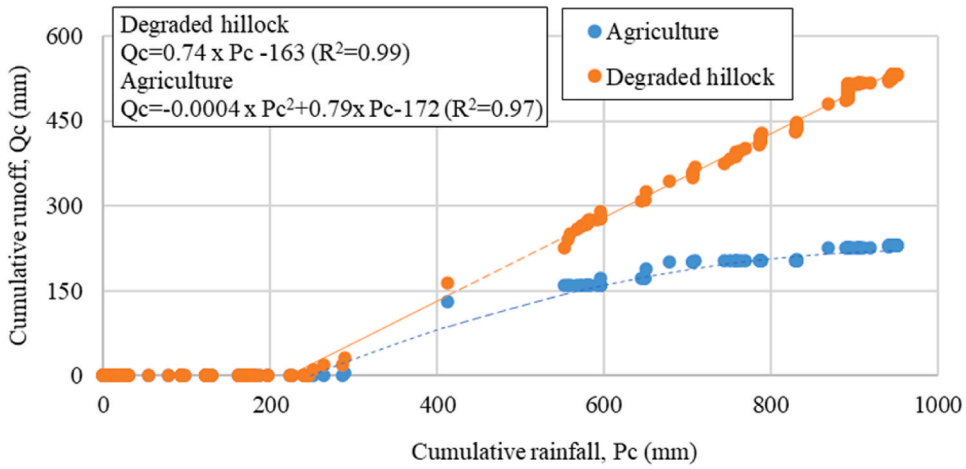

Fig. 6. Runoff measured during 2021-22 from agriculture land and degraded hillock (inflow at S1).

agricultural land has a gentle slope (~1%) and moderate soil depth (50-80 cm). These differences strongly influence runoff generation. To quantify the relationship between rainfall and runoff for each land use type, we developed both linear and polynomial relationships based on measured rainfall and runoff during 2021–22. For the degraded hillock, cumulative runoff (Q_c, in mm) was closely related to cumulative rainfall (P_c, in mm) as:

$$Q_c = 0.74 \times P_c - 163 \quad (R^2 = 0.99) \qquad \text{Eq. 9}$$

For the agricultural land, a second-order polynomial relationship better captured the runoff response:

$$Q_c = -0.0004\,P_c^{\,2} + 0.79\,P_c - 172 \quad (R^2 = 0.97) \qquad \text{Eq. 10}$$

These relationships indicate that degraded hillocks generate runoff at a higher rate per unit rainfall compared to agricultural land, which retains more water due to deeper soils and better infiltration.

Table 2 summarises the measured inflow and outflow at the S1, S2 and S5. S1 and S2 are located at foothills with respective catchment areas of 34 ha and 60 ha whereas S5 is located at the confluence of all stream networks with a total catchment of 116 ha, of which 88.84 ha is degraded land and the 27.16 ha is agricultural land. The total storage capacity created in the S5 catchment was 154,400 m^3 (equivalent to 133 mm). The measured outflow at S1, S2 and S5 was 34%, 26% and 20%, respectively, indicating substantial capture of runoff through decentralized storage. The number of times the storage structures were filled ranged from 2.0 to 3.2 depending on catchment size and storage volume.

3.3. Groundwater recharge

Fig. 7 illustrates the temporal variation in groundwater table measured from 18 observation dug wells between 2018 and 2024, capturing both pre- and post-intervention conditions. Prior to the implementation of landscape resource conservation interventions, groundwater table was generally deep. During 2018-2019, the median groundwater depth during pre-rainy period ranged between 8 and 10 m below ground level (bgl), with individual wells varying by more than 3-4 m because of the prevailing biophysical and topographical heterogeneity.

The first phase of major interventions, including S1 and S2, were implemented between April and June 2019 followed by additional recharge and storage structures in 2020. Following these developments, a notable and sustained improvement in groundwater table was observed. In 2020, the median groundwater depth rose to approximately 2–3 m bgl representing a recovery of nearly 5–7 m compared to pre-intervention conditions. This rise was consistently visible across most wells although the magnitude of recovery spatially varied. Seasonal recharge and its utilization are being clearly reflected in the box-plot distribution. During each *kharif* season, groundwater levels rose sharply followed by gradual drawdown during the *rabi* season and summer months because of irrigation and domestic use. For example, the median groundwater level in 2021 improved from about 6 m bgl in early July to around 2 m bgl by August, indicating rapid recharge driven by rainfall coupled with enhanced infiltration from the landscape interventions. The inter-quartile ranges in the box plots suggest that groundwater response is not uniform across the catchment. Wells located closer to recharge structures, stream channels, and lower landscape positions exhibit larger and faster water table rise, whereas wells located on higher slopes or at elevated parts show comparatively smaller gains. This spatial variability reflects differences in soil depth, fracture density in the hard-rock aquifer and distance from recharge structures. Overall, despite this variability, the median groundwater level across all 18 wells improved by approximately 4–6 m relative to pre-intervention conditions, and this improvement continued through 2024. This

Table 2
Runoff coefficient measured at different outlet points during 2021-22.

Gauging station	Flow accumulation	Cumulative storage capacity created in the catchment (m^3)	Area under Degraded land (ha)	Area under agriculture land (ha)	Total catchment (ha)	Runoff in mm (% of rainfall)	
						Inflow	Outflow
S1	S1	22000	34	-	34	530 (55%)	320 (34%)
S2	S1+S2	48230	60	-	60	402 (42%)	250 (26%)
S3	S3	-		2.8	2.8	-	220 (23%)
S5	S1+S2+S3+S4+S5	154400	88.84	27.16	116	-	191 (20%)

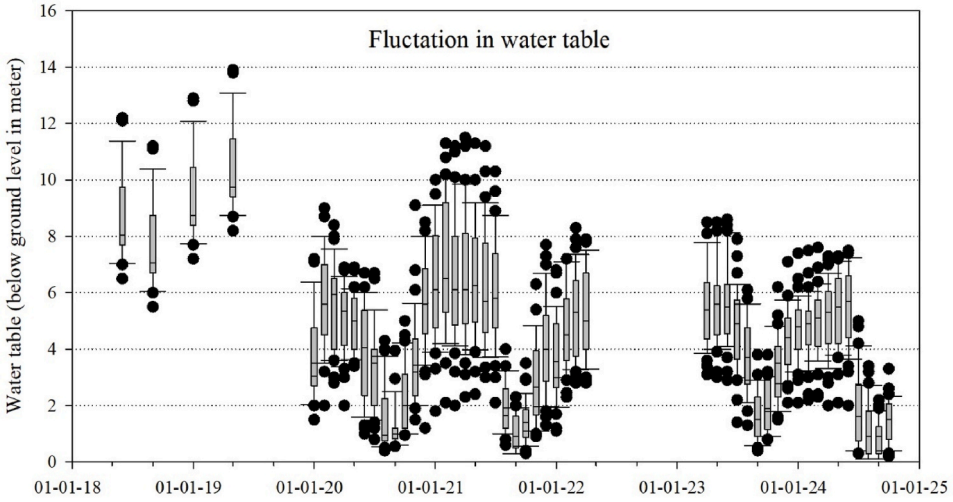

Fig. 7. Fluctuation in water table between 2018 and 2024 (data based on 18 observation dug wells).

improvement in groundwater levels between the pre-intervention (2018–2019) and post-intervention (2020–2024) periods was found to be statistically significant (ANOVA, $p < 0.01$).

The groundwater-level dynamics shown in Fig. 7 were translated to recharge amount, its utilization, and aquifer storage using the WTF method (Table 3). The increase in annual groundwater recharge, net groundwater availability, and carry-over storage after the interventions was statistically significant when compared to the pre-intervention year (ANOVA, $p < 0.01$; Table 3). The sharp post-monsoon rises visible in Fig. 7 correspond to annual recharge increasing from only 20 mm in 2019 to 130 mm in 2020 and further to about 180 mm in 2021, which continued to remain high (>170 mm) during 2022–2023. Importantly, a portion of this recharge was retained as carry-over groundwater storage, which increased from only 5 mm in 2019 to 60 mm in 2021 and further to about 70 mm by 2023, reflecting the sustained elevation of dry-season water levels over the period. This accumulated storage provided a reliable buffer that enabled expansion of irrigation in both *kharif* and *rabi* seasons. Total groundwater use increased from only 7 mm in 2019 to about 167 mm in 2021 and remained around 160 mm by 2023, yet without causing long-term depletion. Instead, net groundwater availability continued to increase, reaching about 240–245 mm after 2021 (Table 3). Stable groundwater levels demonstrate that the landscape interventions transformed the aquifer from a deficit system into a recharge-supported, resilient groundwater system capable of sustaining both agricultural intensification and domestic water security.

Fig. 8 illustrates the plot level groundwater fluctuation recorded by a DIVER installed in one of the observation wells owned by a farmer who is having 2.8 ha of agricultural land (Table 4). The farmer followed a cropping pattern of groundnut–wheat over 2 ha and blackgram–chickpea over the remaining 0.8 ha. Groundnut and blackgram were cultivated during the *kharif* season, while wheat and chickpea were grown during the *rabi* season. To meet the irrigation requirements, the farmer used a 6-horsepower diesel pump set for supplemental irrigation. This well is situated in approximately 50 to 100 m from S1 and S2. Fig. 8 displays continuous measurements of the hydraulic head in the well alongside corresponding rainfall, covering the period from March 2021 to February 2022. During the early part of the monitoring period, rainfall events in May and June led to a gradual rise in the hydraulic head, increasing from approximately 3-4 m. This suggests that even relatively low-intensity rainfall contributed to incremental groundwater recharge.

A high intensity rainfall event of 140 mm was received on July 25, 2021. This triggered a sharp response in the observation well, with the hydraulic head rising from 4 m to 7 m within just few hours. This rapid recharge highlights the improved infiltration and connectivity between surface water structures and the groundwater system, likely enhanced by the landscape resource conservation interventions. Subsequent rainfall events in August and September sustained the elevated groundwater levels. As shown in Fig. 8, the water table rose to 1 m bgl, indicating substantial recharge in the area. By the end of the rainy season in October, groundwater levels began to decline. This decline corresponds with the onset of the *rabi* cropping season, during which farmers started extracting groundwater for irrigation. The drawdown in the hydraulic head, as evident in the figure, reflects this increased water use for agricultural purposes. The pattern clearly demonstrates a balance between natural recharge during the rainy season and groundwater utilization in the post-rainy months.

The analysis indicates that total pumping duration was recorded as 25 h during the *kharif* season and 165 h in the *rabi* season. Majority of the crop water demand during the *kharif* season was met by rainfall. As a result, only one round of supplemental irrigation was applied primarily during the maturity stage of the groundnut crop to facilitate an easier harvest. Additionally, water was pumped for 0.5 to 1.5 h in selected days to meet domestic and livestock needs during this period as indicated by short downward spikes in Fig. 8. In the *rabi* season, the farmer provided 5 to 7 lifesaving supplemental irrigations during the critical growth stages of wheat and chickpea. Each irrigation event lasted pumping water between 1 and 6 h per day, depending on the crop's water requirement and the prevailing weather conditions. This intensive irrigation schedule in the *rabi* season contributed significantly to the higher total pumping hours observed. The DIVER data further supports that despite continuous pumping, particularly during the *rabi* season, the storage wells exhibited rapid recovery with water levels returning to their original state within the same day. This quick recovery can be primarily attributed to the consistent availability of subsurface water flow, which is supported by the storage and gradual release of water from the treated catchment and quick returned flow of irrigated water. Similarly, data collected from cropping system and pumping hours using DIVER pressure transducers in four different plots for the year 2021-22 is summarised in Table 4. Farmers having agricultural land of 1.4-2.8 ha could support different cropping system such as groundnut, blackgram in *kharif* season and wheat, mustard, chickpea, barley in *rabi* season. The average pumping hours with a 6 hp diesel pump were 16.5 h and 56 h ha^{-1} during *kharif* and *rabi* season, respectively. In addition, Average energy consumption during *kharif* and *rabi* season was 74 KWH ha^{-1} and 250 KWH ha^{-1}, respectively.

Table 3
Change in key ecosystem services along with impact indicators.

SN	Indicators	2019	2020	2021	2023	Statistical significance
A	**Groundwater balance**					
	Carry forward groundwater storage from previous year (mm)	5	10	60	70	
	Groundwater recharge (mm)	20	130	180	175	*** ($p < 0.01$)
	Net Groundwater availability (mm)	25	140	240	245	***
	Net irrigation use in *kharif* (mm)	1	11	25	24	***
	Net irrigation use in *rabi* (mm)	6	58	142	136	***
	Total groundwater use for agriculture (mm)	7	69	167	160	***
B	**Crop yield (Kg ha^{-1})**					
	Groundnut (*Kharif*)	1250 (450)	1460 (270)	1350 (340)	1540 (230)	** ($p < 0.05$)
	Black gram (*kharif*)	350 (130)	450 (135)	380 (140)	335 (230)	ns
	Wheat (*rabi*)	1580 (350)	3050 (450)	3550 (380)	3470 (380)	***
	Chickpea (*rabi*)	450 (230)	1250 (460)	1470 (230)	1450 (330)	***
C	**Income from Agriculture (USD)**					
	Net income during *kharif* (USD)	790	8300	24700	27500	***
	Net income during *rabi* (USD)	1580	27600	79000	86800	***
	Net income: Livestock (USD)	-	2650	13200	34200	
	Net income/year (USD)	2370	38550	116900	148500	***
	Net income/HH/year	52	856	2597	3300	***
D	**Socio-economic status**					
	Well recovery period (hours)	120	20	10	10	***
	Drinking water availability (months)	4-5	12	12	12	
	In-migration (no. of families)	-	15	45	45	
	Children's registration in school	-	4	14	15	
	No of hours women engaged for domestic water	3-4	<1	<1	<1	

Values in parentheses represent the standard deviation (SD) of the mean; Statistical significance refers to comparison between pre-intervention (2019) and post-intervention (2020–2023) periods. Continuous variables were tested using one-way ANOVA. ***$p < 0.01$, **$p < 0.05$; ns = not significant ($p \geq 0.05$).

3.4. Crop intensification

To assess the impact of landscape-level resource conservation on crop intensification, both satellite-based NDVI values were analysed along with the intensive field-based observations. The NDVI data for February (representing peak *rabi* season vegetation cover) were extracted for the period 2018–2023 (Fig. 9), where 2018 represented the pre-intervention baseline data and 2019–2023 corresponded to the intervention and post-intervention periods. Agricultural plots within the 250 ha watershed were delineated using geospatial field boundaries covering 121 ha of cultivable land. In parallel, detailed ground-truthing was undertaken for all agricultural fields by dividing the cultivable area into 185 field parcels and recording crop type and cropped area during each *kharif* and *rabi* season from 2018 to 2023 (Fig. 10 a,b). This parcel-level survey provided accurate estimates of cropped area and seasonal crop distribution, which were further validated using NDVI-based vegetation maps.

Prior to the implementation of conservation interventions in 2018, only about 4 ha of land was cultivated in both *kharif* and *rabi* seasons with most fields remaining fallow due to severe water scarcity. Following the construction of decentralized rainwater harvesting structures and groundwater recharge, cropped area increased to 35 ha in 2019 and expanded rapidly after 2020, reaching 95–110 ha by 2021–2022 (Fig. 10). This expansion occurred in both seasons, indicating a transition from limited rainfed cultivation to more intensive and reliable double-cropping systems. In addition to the increase in cultivated area, the interventions also led to a clear shift in crop composition and diversification. During the *kharif* season, cultivation in 2018–2019 was dominated by fallow land with only small areas under sesame and groundnut. After improved water availability, groundnut became the dominant *kharif* crop from 2020 onward, followed by blackgram and sesame. Vegetable cultivation, which was nearly absent before the interventions, also emerged after 2021, reflecting increased soil moisture, groundwater availability, and farmers' willingness to consume vegetable crops for their own use. A similar transformation occurred in the *rabi* season. Before the interventions, almost the entire agricultural area remained fallow due to lack of irrigation. From 2020 onwards, wheat became the dominant *rabi* crop, occupying more than 60% of the cultivated area by 2021–2022. Chickpea and mustard also expanded gradually, while vegetables appeared as a minor but increasing component. This shift from fallow and single-season cropping to irrigated, diversified double-cropping systems demonstrates the strong influence of decentralized water harvesting and groundwater recharge on agricultural intensification. The NDVI maps (Fig. 9) also show a clear increase in vegetation cover and spatial continuity of cropped land after 2020, consistent with the field-measured expansion of cultivated area and crop diversity. Together, the field-based crop parcel data and satellite-derived NDVI provide robust evidence that landscape resource conservation significantly enhanced cropping intensity and land productivity in the watershed.

3.5. Crop yield, household income and socio-economic impact

Table 3 shows the changes in crop productivity, farm income, and socio-economic conditions following the implementation of landscape resource conservation interventions. Improvements in water availability, cropping intensity, and irrigation reliability resulted in substantial gains in agricultural production and household livelihoods. Crop yields increased consistently across both *kharif* and *rabi* seasons. During the *kharif* season, groundnut yield increased from 1250 kg ha^{-1} in 2019 to 1540 kg ha^{-1} in 2023, while blackgram yield rose from 350 to 435 kg ha^{-1}. In the *rabi* season, wheat yield more than doubled, increasing from 1580 kg ha^{-1} in 2019 to 3670 kg ha^{-1} in 2023, and chickpea yield increased from 450 to about 1460 kg ha^{-1}. These yield gains reflect improved soil moisture conditions and the availability of assured irrigation from recharged groundwater, allowing timely sowing and better crop management. The increases in crop yields across both *kharif* and *rabi* seasons after the interventions were statistically significant when compared to the pre-intervention year (ANOVA, $p < 0.05$; Table 3). The combined effects of yield improvement and crop intensification resulted in a sharp increase in farm income. In 2019, the total annual net income from agriculture (from entire cluster) was only USD

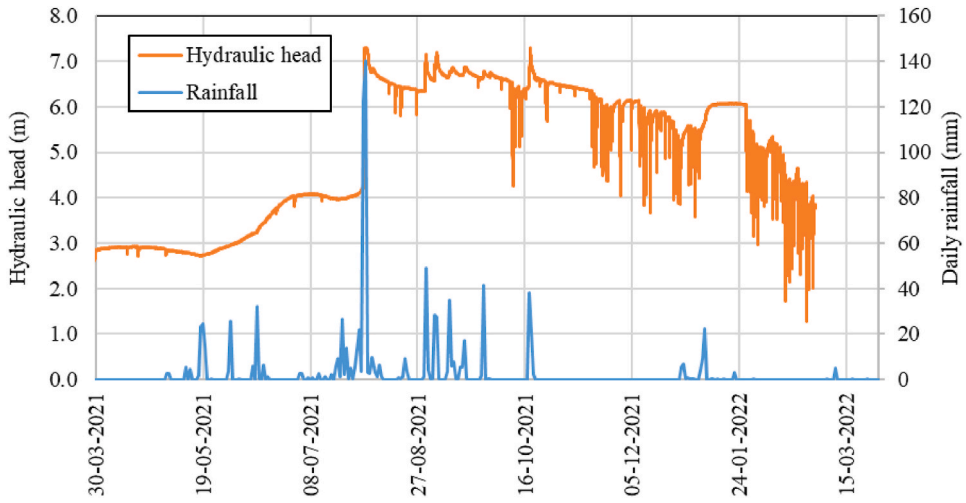

Fig. 8. Groundwater recharge and utilization pattern of a selected well during 2021-22.

Table 4
Pumping hours, energy consumption and amount of irrigation applied in selected plots during *kharif* and *rabi* season.

Plot no	Cropping system		Pumping hours using 6 HP diesel pump		Amount of irrigation applied using flood methods (mm)	
	Area cultivated in *kharif*	Area cultivated in *rabi*	During *kharif*	During *rabi*	During *kharif*	During *rabi*
1[a]	Groundnut: 2 Ha Black gram: 0.8 Ha	Wheat: 2 Ha Mustard: 0.4 Ha Chickpea:0.4 Ha	25	165	155	1030
2	Groundnut: 2.4 Ha Fallow: 0.8 Ha	Wheat: 3 Ha Chickpea: 0.2 Ha	34	182	250	990
3	Groundnut: 1.2 Ha Black gram: 0.4 Ha	Wheat: 0.8 Ha Barley: 0.4 Ha Chickpea: 0.2 Ha Mustard: 0.2 Ha	24	63	260	690
4	Groundnut: 0.8 Ha Fallow: 0.6 Ha	Wheat: 0.8 Ha Mustard: 0.2 Ha Fallow: 0.4 Ha	23	92	500	1600
Average pumping hours using 6HP diesel pump set			16.5 Hours ha^{-1}	56 Hours ha^{-1}		
Average Energy consumption			74 KWH ha^{-1}	250 KWH ha^{-1}		
Average irrigation amount (mm)					260	1050

[a] Details regarding groundwater dynamics has been provided in Fig. 8.

2,370, comprising USD 790 from *kharif* crops and USD 1580 from *rabi* crops, with negligible contribution from livestock. With the expansion of cropped area and the introduction of double cropping, total annual net income increased to USD 38,550 in 2020 and further to USD 116,900 in 2021 at the cluster scale. By 2023, total net income from *kharif* crops reached USD 27,500, *rabi* crops USD 86,800, and livestock USD 34,200, resulting in a total annual net income of USD 148,500 at the cluster scale. Consequently, the average household income increased from only USD 52 $year^{-1}$ in 2019 to approximately USD 3300 $year^{-1}$ in 2023. The increase in total agricultural income at the cluster level following the implementation of landscape resource conservation measures was found to be statistically significant (ANOVA, $p < 0.01$; Table 3).

Socio-economic conditions improved markedly alongside rising incomes. The recovery period of wells declined from about 120 h in 2019 to 10 h by 2021, indicating enhanced groundwater recharge and well sustainability. Changes in well recovery time and well-functioning status before and after interventions were also statistically significant based on Chi-square analysis ($p < 0.01$). Drinking water availability improved from only 4–5 months per year to year-round availability. These changes significantly reduced the time women spent collecting domestic water, from 3 to 4 h per day in 2019 to less than 1 h after 2020. Improved livelihood security also led to a reversal of migration trends. No return migration was recorded in 2019; however, 15 families returned by 2020, and a total of 45 families had returned by 2021, a level that remained stable through 2023. Improved household stability was further reflected in increasing school enrolment, which rose from zero in 2019 to 15 children by 2023. Overall, the results demonstrate that improved water availability and agricultural productivity substantially strengthened rural livelihoods and socio-economic well-being in the study watershed.

4. Discussion

The landscape restoration efforts significantly altered hydrologic responses within the watershed, particularly in terms of rainfall-runoff relationships and water retention. The construction of water harvesting structures particularly in uplands enabled effective capture and management of surface runoff. Notably, 55% of the rainfall received by the degraded hillock catchment was converted into runoff, yet approximately 210 mm of this was retained within the structure before any spill-over occurred. This demonstrates enhanced water retention capacity that delays and reduces runoff, helping to improve soil moisture. Furthermore, the consistent infiltration rates (18–22 mm day^{-1}) observed across rainy season reflect a stable and functional hydrologic system, likely supported by the strategic positioning of reservoirs in areas with favorable hydraulic gradients (Ellison et al. 2017; Kourakos et al. 2019; Hiscock et al. 2024). The comparative analysis of runoff from different land uses reinforced these findings, revealing that degraded hillocks contributed significantly more runoff than agricultural lands

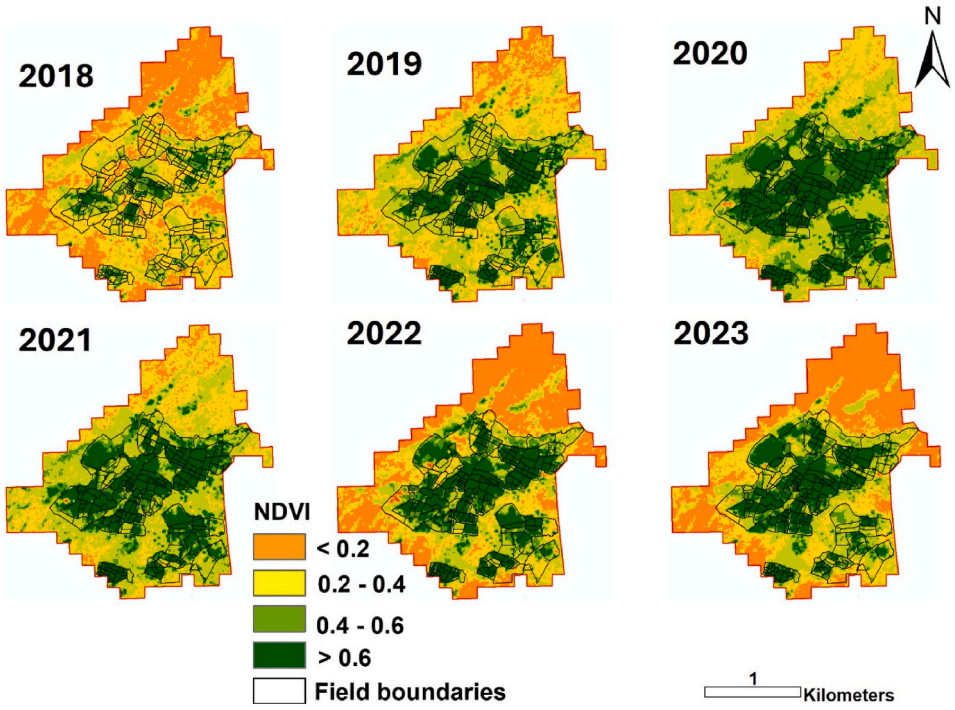

Fig. 9. NDVI mapping indicating crop intensification between 2018 and 2023.

due to shallow soils and sparse vegetation (Zhang et al. 2025). This suggests that targeted land use improvements are key for managing runoff and improving water availability.

Post-intervention monitoring of groundwater levels revealed a substantial and rapid recharge response, driven by improved surface water capture and infiltration. Groundwater depths that previously exceeded 9 m below ground level during pre-intervention years were significantly reduced to as little as 1.2 m within 2-3 years of implementing watershed structures. The temporal alignment of rainfall events with swift rises in hydraulic head especially during high-intensity storms indicates improved connectivity between surface water and the aquifer system (Liu et al. 2025). Even during periods of active pumping for irrigation, water tables recovered quickly, underscoring the sustainability of water usage in the post-intervention landscape. These changes collectively highlight the role of landscape restoration in stabilizing local hydrology, ensuring year-round water availability, and reducing vulnerability to drought conditions (Stanturf, 2021; Constenla-Villoslada et al. 2022; Kebede et al. 2023; Nedbal et al. 2025). The magnitude of groundwater recharge closely matches the volume of runoff harvested. While about 210 mm of runoff was captured in surface structures, nearly 180 mm was realized as effective groundwater recharge (Table 3), indicating that most of the harvested water was transferred to aquifer storage.

The improved hydrologic conditions translated directly into increased agricultural activity and crop productivity. NDVI analysis along with ground survey indicated that agricultural intensification expanded the actively cultivated area from just 4 ha in 2018 to over 100 ha by 2023. This change was facilitated by reliable groundwater access, reduced surface runoff, and better soil moisture retention factors that enabled both *kharif* and *rabi* season cultivation. Farmers were able to implement more diverse and intensive cropping patterns, including staple crops such as wheat, chickpea, and groundnut, supported by supplemental irrigation drawn from improved groundwater stores. The availability of water throughout the year also allowed for lifesaving irrigation during critical crop growth stages, directly contributing to higher yields and reduced crop failure risks (Deb et al. 2022). Overall, restoration practices not only supported agricultural expansion but also improved the productivity and resilience of the farming system. This additional groundwater storage, created by only about 200 mm of harvested runoff, was sufficient to support two cropping seasons in an area that was previously largely fallow. Thus, a relatively modest hydrologic intervention translated into a complete shift from rainfed fallow systems to double-cropped irrigated agriculture.

Groundwater was the sole source of irrigation in the study cluster and was utilized using diesel pump sets from shallow dug wells. Irrigation water was applied through traditional flood irrigation methods, which are dominant in the region. On average, 260 mm and 1050 mm of supplemental irrigation were applied during *kharif* and *rabi*, respectively. However, although large volumes of groundwater were pumped and applied to fields, a substantial fraction of this water did not leave the hydrologic system. As the soils are coarse textured, applied irrigation water rapidly infiltrates beyond the root zone, generating significant return flow to the shallow aquifer. Earlier studies in similar hard-rock, sandy agro-ecosystems have shown that 70–80% of applied irrigation water returns to groundwater through deep percolation, particularly when flood irrigation is practiced on coarse-textured soils (Bailey, 2025). This strong return flow explains how high irrigation use ($>$1200 mm yr^{-1} at plot scale) could be sustained for crop intensification at the cluster level. The combination of rainwater harvesting–induced recharge (105–180 mm yr^{-1}) and irrigation return flow maintained and even increased carry-forward groundwater storage (from 5 mm in 2019 to 70 mm in 2023). Thus, groundwater pumping for agriculture did not represent a net loss from the system; rather, it functioned as an internal recycling mechanism within a recharge-enhanced aquifer, enabling high irrigation depths to coexist with sustained groundwater availability.

The restoration of natural resources significantly improved the socio-economic conditions of the community. With better water availability and enhanced farming conditions, migration trends were reversed, and 45 families comprising 248 individuals those returned to their villages to resume agricultural activities. The reduction in fallow land from 117 ha in 2019 to only 11 ha in 2023 is a key indicator of this transformation. Households that once faced livelihood insecurity due to water scarcity are now engaging in productive farming and livestock rearing. As a result, total annual net income at cluster scale from agriculture and

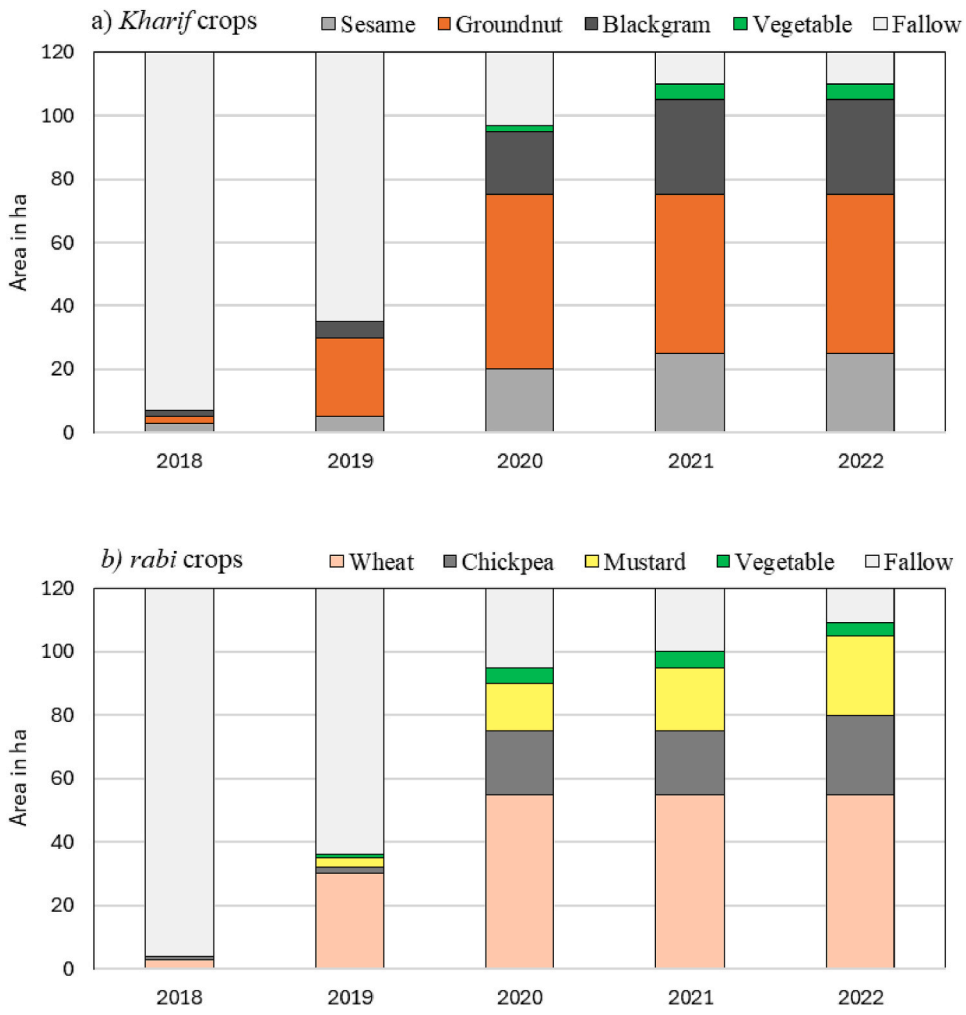

Fig. 10. Temporal changes in cropping pattern and cultivated area during *kharif* and *rabi* seasons following landscape restoration (2018–2022).

allied activities surged from just USD 2370 in 2019 to USD 148,500 in 2023. This remarkable increase reflects not only a revival of rural economy but also a broader uplift in living standards and socio-economic resilience. Beyond income generation, these integrated landscape interventions have contributed meaningfully to local food security and sustainable development (Estrada-Carmona et al., 2024). The expansion of cultivated land and the intensification of cropping cycles have increased local food availability, reducing dependence on external food sources. The rise in average household income to approximately USD 3300 well above the rural national average underscores the interventions' contribution to poverty alleviation and improved living conditions. These outcomes demonstrate that ecosystem restoration, when paired with community-based water and land management, can serve as a powerful lever for achieving environmental sustainability alongside socio-economic development (Sayer et al. 2013; Freeman et al. 2015; Reed et al 2017, 2021).

To address the complex and interconnected challenges of land degradation, restoration, and agricultural sustainability, there is an urgent need for integrated, multidisciplinary research. This should aim to generate scalable knowledge that links ecological processes with socio-economic outcomes, thereby guiding the design of restoration interventions that not only rehabilitate the environment but also enhance rural livelihoods and food security. By understanding the hydrologic, ecological, and socio-economic impacts of landscape restoration across different spatial scales, we can better inform policy and practice aimed at reversing degradation, improving water productivity, and building resilience in vulnerable agricultural systems.

5. Conclusions

This study demonstrates the transformative impact of integrated landscape restoration and water conservation measures on hydrologic processes, agricultural productivity, and rural livelihoods in a semi-arid watershed. The construction of water harvesting structures in decentralized manner, particularly in uplands, significantly improved water retention capacity of the landscape. Key hydrologic outcomes include a reduction in surface runoff, delayed spillover thresholds, and a consistent infiltration rate throughout the rainy season. These changes not only reduced water loss but also facilitated substantial groundwater recharge with about 210 mm of runoff harvested within the structures translating into 105-180 mm y^{-1} of net groundwater recharge, as evidenced by the sharp rise in water table levels and the rapid recovery of observation wells after irrigation withdrawals.

The improved hydrologic regime directly supported the intensification of agriculture within the catchment. Cultivated area expanded from a mere 4 ha to over 110 ha within three years, enabled by enhanced soil moisture and reliable groundwater access. This additional recharge of roughly 180 mm, generated from landscape-scale runoff harvesting, was sufficient to sustain two cropping seasons on lands that were previously permanent fallows. Farmers adopted diversified cropping systems with

both *kharif* and *rabi* season cultivation, supported by supplemental irrigation. This shift not only improved food production and reduced fallow land but also enhanced the resilience of local agriculture to climatic variability.

Equally important are the socio-economic benefits observed as a result of these interventions. The increased availability of water and the revitalization of agriculture reversed distress migration and encouraged the return of 45 families to their native village. Total annual net incomes at cluster scale improved significantly, rising from USD 2370 in 2019 to USD 148,500 in 2023. The average income per household now exceeds the national rural average, reflecting improved livelihoods, reduced vulnerability, and enhanced food security. Importantly, intensive groundwater use did not lead to depletion because flood-irrigated, coarse-textured soils returned 70–80% of applied water back to the shallow aquifer, reinforcing the recharge created by rainwater harvesting.

While this study relies on intensive field monitoring and a robust before–after assessment, further refinement through longer-term observations and comparative treated–untreated watershed studies would strengthen attribution of hydrologic and livelihood outcomes. Such efforts will also help capture additional processes such as evapotranspiration and soil moisture dynamics across varied agro-ecological settings. Overall, the findings affirm that integrated landscape resource conservation measures, centred on natural resource restoration and community participation, can yield synergistic benefits for hydrology, agriculture, and rural development. Such models offer scalable solutions for addressing the twin challenges of land degradation and rural poverty in water-stressed regions. Further empirical evidence from comparative studies in treated and untreated watersheds across different agro-ecological contexts will strengthen the understanding of intervention impacts and support the design of scalable pathways to revert degraded lands into productive landscapes. Continued monitoring and adaptive management will be essential to sustaining these gains and ensuring long-term ecological and socio-economic resilience. The approach presents a replicable pathway toward sustainable development goals related to water security, climate resilience, and inclusive rural growth.

CRediT authorship contribution statement

Venkata Radha Akuraju: Conceptualization, Data curation, Methodology, Writing – original draft. **Kaushal K. Garg:** Conceptualization, Data curation, Formal analysis, Methodology, Supervision, Writing – original draft. **K.H. Anantha:** Conceptualization, Methodology, Writing – original draft. **Shishuvendra Kumar:** Data curation, Investigation, Methodology. **Ashok Shukla:** Data curation, Methodology. **Ramesh Singh:** Conceptualization, Project administration, Validation. **Bhabani Sankar Das:** Methodology, Writing – review & editing. **M.L. Jat:** Methodology, Writing – review & editing.

Declaration of competing interest

The authors declare that they have no known competing financial interests or personal relationships that could have appeared to influence the work reported in this paper.

Acknowledgements

The authors gratefully acknowledge the financial support provided by the Government of Uttar Pradesh for the development of model watersheds in the Bundelkhand region during the period 2018 to 2022 under the Rashtriya Krishi Vikas Yojana (RKVY). The authors also extend their appreciation to the One CGIAR initiative, particularly the *Multifunctional landscape* mega program, for supporting a portion of the scientific staff time, which significantly contributed to the interdisciplinary research efforts documented in this work.

Data availability

Data will be made available on request.

References

Anantha, K.H., Garg, K.K., Barron, J., Dixit, S., Venkataradha, A., Singh, R., Whitbread, A., M, 2021c. Impact of best management practices on sustainable crop production and climate resilience in smallholder farming systems of South Asia. Agric. Syst. 194, 103276. https://doi.org/10.1016/j.agsy.2021.103276.

Anantha, K.H., Garg, K.K., Moses, S.D., Patil, M.D., Sawargaonkar, G.L., Kamdi, P.J., Malve, S., Sudi, R., Raju, K.V., Wani, S.P., 2021b. Impact of natural resource management interventions on water resources and environmental services in different agroecological regions of India. Groundw. Sustain. Dev. 13, 100574. https://doi.org/10.1016/j.gsd.2021.100574.

Anantha, K.H., Garg, K.K., Petrie, C.P., Dixit, S., 2021a. Seeking sustainable pathways for fostering agricultural transformation in peninsular India. Environ. Res. Lett. 16, 044032. https://doi.org/10.1088/1748-9326/abed7b.

Anantha, K.H., Garg, K.K., Singh, R., Venkataradha, A., Dev, I., Petrie, C.A., Whitbread, A.M., Dixit, S., 2022. Landscape resource management for sustainable crop intensification. Environ. Res. Lett. 17, 014006. https://doi.org/10.1088/1748-9326/ac413a.

Bailey, R.T., 2025. Quantifying hydrologic fluxes in an irrigated region characterized by groundwater return flows. J. Hydrol. 648, 132402.

Barbier, E.B., Hochard, J.P., 2018. Land degradation and poverty. Nat. Sustain. 1, 623–631.

Constenla-Villoslada, S., Liu, Y., Wen, J., Sun, Y., Chonabayashi, S., 2022. Large-scale land restoration improved drought resilience in Ethiopia's degraded watersheds. Nat. Sustain. 5, 488–497. https://doi.org/10.1038/s41893-022-00861-4.

de Graaf, I.E.M., Gleeson, T., Rens) van Beek, L.P.H., Sutanudjaja, E.H., Bierkens, M.F.P., 2019. Environmental flow limits to global groundwater pumping. Nature 574, 90–94.

Deb, P., Moradkhani, H., Han, X., Abbaszadeh, P., Xu, L., 2022. Assessing irrigation mitigating drought impacts on crop yields with an integrated modeling framework. J. Hydrol. 609, 127760. https://doi.org/10.1016/j.jhydrol.2022.127760.

Deng, Q., Sharretts, T., Ali, T., Zoe Ao, Y., Chiarelli, D.D., Demeke, B., Marston, L., Mehta, P., Mekonnen, M., Rulli, M.C., Tuninetti, M., Xie, W., Davis, K.F., 2025. Deepening water scarcity in breadbasket nations. Nat. Commun. 16, 1110. https://doi.org/10.1038/s41467-025-56022-6.

Dewandel, B., Perrin, J., Ahmed, S., Aulong, S., Hrkal, Z., Lachassagne, P., Samad, M., Massuel, S., 2010. Development of a tool for managing groundwater resources in semi-arid hard rock regions: application to a rural watershed in South India. Hydrol. Process. 24, 2784–2797.

Dinar, A., Tieu, A., Huynh, H., 2019. Water scarcity impacts on global food production. Global Food Secur. 23, 212–226.

Ellison, D., Morris, C.E., Locatelli, B., Sheil, D., Cohen, J., Murdiyarso, D., Gutierrez, V., van Noordwijk, M., Creed, I.F., Pokorný, J., Gaveau, D., Spracklen, D.V., Tobella, A. B., Ilstedt, U., Teuling, A.J., Gebrehiwot, S.G., Sands, D.C., Muys, B., Verbist, B., et al., 2017. Trees, forests and water: cool insights for a hot world. Glob. Environ. Change 43, 51–61. https://doi.org/10.1016/j.gloenvcha.2017.01.002.

Elsu, C.A., Ramesh, K.V., Sridevi, H., 2017. Quantification and understanding the observed changes in land cover patterns in Bangalore. Int. J. Civ. Eng. Technol. 8, 597–603.

Estrada-Carmona, N., Carmenta, R., Reed, J., Betemariam, E., DeClerck, F., Falk, T., Hart, A.K., Jones, S.K., Kleinschroth, F., McCartney, M., et al., 2024. Reconciling conservation and development requires enhanced integration and broader aims: a cross-continental assessment of landscape approaches. One Earth 7, 1858–1873.

Famiglietti, J., 2014. The global groundwater crisis. Nat. Clim. Change 4, 945–948.

Feng, L., Wang, Y., Fensholt, R., Tong, X., Tagesson, T., Zhang, X., Ardö, J., Zhou, J., Shao, W., Dou, Y., Sang, Y., Tian, F., 2025. Globally increased cropland soil exposure to climate extremes in recent decades. Nat. Commun. 16, 4354. https://doi.org/10.1038/s41467-025-59544-1.

Ferrant, S., Oehler, F., Durand, P., Justes, E., Gascuel-Odoux, C., Garnier, F., Grimaldi, C., Gruhier, C., Masson, E., Probst, A., Probst, J.L., Prudent, P., 2014. Simulation of land use change and water balance in a Mediterranean agricultural watershed. Environ. Earth Sci. 72, 3881–3894. https://doi.org/10.1007/s12665-014-3289-5.

Fitton, N., Smith, P., Alexander, P., Arnell, N., Bajzelj, B., Calvin, K., Doelman, J., Stehfest, E., Gerber, J.S., West, P.C., Havlik, P., Krisztin, T., Hasegawa, T., Herrero, M., van Meijl, H., Powell, T., Sands, R., 2019. The vulnerabilities of agricultural land and food production to future water scarcity. Glob. Environ. Change 58, 101944.

Food and Agriculture Organization (FAO), 2019. *The State of the World's Biodiversity for Food and Agriculture*. Commission on Genetic Resources for Food and Agriculture Assessments. FAO. https://www.fao.org/3/CA3129EN/ca3129en.pdf.

Freeman, O.E., Duguma, L.A., Minang, P.A., 2015. Operationalizing the integrated landscape approach in practice. Ecol. Soc. 20, 24.

Frisbee, M.D., Caffee, M.W., Camberato, J.J., Michalski, G., 2022. Using multiple isotopic and geochemical tracers to disentangle the sources of baseflow and salinity in the headwaters of a large agricultural watershed. J. Hydrol. 609, 127769.

Garg, K.K., Akuraju, V., Anantha, K.H., Singh, R., Whitbread, A.M., Dixit, S., 2022. Identifying potential zones for rainwater harvesting interventions for sustainable intensification in the semi-arid tropics. Sci. Rep. 12, 3882. https://doi.org/10.1038/s41598-022-07847-4.

Garg, K.K., Anantha, K.H., Nune, R., Venkataradha, A., Singh, P., Gumma, M.K., Dixit, S., Ragab, R., 2020b. Impact of land use changes and management practices on groundwater resources in Kolar district, southern India. J. Hydrol. Reg. Stud. 31, 100732. https://doi.org/10.1016/j.ejrh.2020.100732.

Garg, K.K., Singh, R., Anantha, K.H., Singh, A.K., Akuraju, V.R., Barron, J., Dev, I., Tewari, R.K., Wani, S.P., Dhyani, S.K., Dixit, S., 2020a. Building climate resilience in degraded agricultural landscapes through water management: a case study of Bundelkhand region, Central India. J. Hydrol. 591, 125592. https://doi.org/10.1016/j.jhydrol.2020.125592.

Gashaw, T., Tulu, T., Argaw, M., Worqlul, A.W., 2018. Land use/land cover change and its impact on ecosystem services in the central highlands of Ethiopia. Remote Sens. Appl.: Society and Environment 10, 133–142. https://doi.org/10.1016/j.rsase.2018.03.001.

Gleeson, T., Wada, Y., Bierkens, M.F.P., van Beek, L.P.H., 2012. Water balance of global aquifers revealed by groundwater footprint. Nature 488, 197–200.

Glendenning, C.J., Vervoort, R.W., 2010. Hydrological impacts of rainwater harvesting (RWH) in a case study catchment: the Arvari River, Rajasthan, India. Part 1: field-scale impacts. Agric. Water Manag. 98, 331–342.

Hiscock, K.M., Balashova, N., Cooper, R.J., Bradford, P., Patrick, J., Hullis, M., 2024. Developing managed aquifer recharge (MAR) to augment irrigation water resources in the sand and gravel (Crag) aquifer of coastal Suffolk, UK. J. Environ. Manag. 351, 119639. https://doi.org/10.1016/j.jenvman.2023.119639.

Intergovernmental Science-Policy Platform on Biodiversity and Ecosystem Services (IPBES), 2018. In: Montanarella, L., Scholes, R., Brainich, A. (Eds.), The IPBES Assessment Report on Land Degradation and Restoration. IPBES Secretariat.

Kebede, W., Temesgen, B., Getachew, F., Girma, F., Gessesse, G., Damitew, F., 2023. Towards sustainable watershed-based landscape restoration in degraded drylands: perceived benefits and innovative pathways learnt from project-based interventions in Ethiopia. J. Environ. Manag. 335, 117499.

Keesstra, S.D., Bouma, J., Wallinga, J., Tittonell, P., Smith, P., Cerdà, A., Montanarella, L., Quinton, J.N., Pachepsky, Y., van der Putten, W.H., Bardgett, R.D., Moolenaar, S., Mol, G., Jansen, B., Fresco, L.O., 2018. The significance of soils and soil science towards realization of the United Nations Sustainable Development Goals. SOIL 4, 157–162. https://doi.org/10.5194/soil-4-157-2018.

Khosravi Mashizi, A., Sharafatmandrad, M., 2025. Spatial management of poverty-biodiversity interactions in semi-arid ecosystems. Sci. Rep. 15, 19802.

Kourakos, G., Dahlke, H.E., Harter, T., 2019. Increasing groundwater availability and seasonal base flow through agricultural managed aquifer recharge in an irrigated basin. Water Resour. Res. 55, 7464–7492.

Leal Filho, W., Shiel, C., Paço, A., Brandli, L.L., 2019. The role of transformation in learning and education for sustainable development. J. Clean. Prod. 199, 618–629. https://doi.org/10.1016/j.jclepro.2018.07.017.

Lipper, L., Thornton, P., Campbell, B.M., Baedeker, T., Braimoh, A., Bwalya, M., Caron, P., Cattaneo, A., Garrity, D., Henry, K., Hottle, R., Jackson, L., Jarvis, A., Kossam, F., Mann, W., McCarthy, N., Meybeck, A., Neufeldt, H., Remington, T., Wollenberg, E., 2017. Climate-smart agriculture for food security. Nat. Clim. Change 4, 1068–1072. https://doi.org/10.1038/nclimate2437.

Liu, H., Yan, H., Guan, M., 2025. Evaluating the effects of topography and land use change on hydrological signatures: a comparative study of two adjacent watersheds. Hydrol. Earth Syst. Sci. 29, 2109–2132.

MacDonald, G.K., Brauman, K.A., Sun, S., Carlson, K.M., Cassidy, E.S., Gerber, J.S., West, P.C., 2016. Rethinking agricultural trade relationships in an era of globalization. Nat. Plants 2, 16065. https://doi.org/10.1038/nplants.2016.65.

Mansour, L., Rowntree, K., Grenfell, M., 2022. Assessing landscape restoration outcomes for hydrology and livelihoods: a systematic review. Ecol. Indic. 135, 108564. https://doi.org/10.1016/j.ecolind.2021.108564.

Mitra, A., Rao, N., 2019. Gender, water, and nutrition in India: an intersectional perspective. Water Altern. (WaA) 12, 169–191.

Montanarella, L., Pennock, D.J., McKenzie, N., Badraoui, M., Chude, V., Baptista, I., Mamo, T., Yemefack, M., Aulakh, M.S., Yagi, K., Hong, S.Y., Vijarnsorn, P., Zhang, G. L., Arrouays, D., Black, H., Krasilnikov, P., Sobocká, J., Alegre, J., Henriquez, C.R., Vargas, R., 2016. World's soils are under threat. SOIL 2, 79–82. https://doi.org/10.5194/soil-2-79-2016.

Nedbal, V., Bernasová, T., Kobesová, M., Tesařová, B., Vácha, A., Brom, J., 2025. Impact of landscape management and vegetation on water and nutrient runoff from small catchments for over 20 years. J. Environ. Manag. 373, 123748. https://doi.org/10.1016/j.jenvman.2024.123748.

NITI Aayog, 2016. Human Development Report, Bundelkhand Human Development Report 2012. Prepared under NITI Aayog-UNDP Project on Human Development: Towards bridging inequalities, p. 258.

Nkonya, E., Mirzabaev, A., von Braun, J. (Eds.), 2016. Economics of Land Degradation and Improvement: a Global Assessment for Sustainable Development. Springer. https://doi.org/10.1007/978-3-319-19168-3.

Olsson, L., Barbosa, H., Bhadwal, S., Cowie, A., Delusca, K., Flores-Rentería, D., Hermans, K., Jobbagy, E., Kurz, W., Li, D., Martino, D., McIntyre, T., Ndegwa, G., Stringer, L.C., 2019. Land degradation. In: IPCC Special Report on Climate Change and Land. https://www.ipcc.ch/srccl/.

Padhan, N., Anantha, K.H., Garg, K.K., Akuraju, V., Singh, R., Jat, M.L., 2025. Interplay of resource endowments, agriculture and nutritional outcomes in the Central Indian Landscape. Front. Sustain. Food Syst. 9, 1596474. https://doi.org/10.3389/fsufs.2025.1596474.

Pal, S.C., Chatterjee, U., Chakrabortty, R., Roy, P., Chowdhuri, I., Saha, A., Abu, Reza Md, Islam, T., Edris, Alam, Md Kamrul, Islam, 2023. Anthropogenic drivers induced desertification under changing climate: issues, policy interventions, and the way forward. Prog. Disaster Sci. 20, 100303.

Plassin, S., Koch, J., Wilson, M., Neal, K., Friedman, J.R., Paladino, S., Worden, J., 2021. Multi-scale fallow land dynamics in a water-scarce basin of the U.S. Southwest. J. Land Use Sci. 16, 291–312. https://doi.org/10.1080/1747423X.2021.1928310.

Rantz, S.E., 1982. Measurement and computation of streamflow: volume 2—Computation of discharge. U. S. Geol. Surv. Water Supply Pap., 2175

Reed, J., Kusters, K., Barlow, J., Balinga, M., Borah, J.R., Carmenta, R., Chervier, C., Djoudi, H., Gumbo, D., Laumonier, Y., Moombe, K.B., Yuliani, E.L., Sunderland, T., 2021. Re-integrating ecology into integrated landscape approaches. Landsc. Ecol. 36, 2395–2407.

Reed, J., van Vianen, J., Barlow, J., Sunderland, T., 2017. Have integrated landscape approaches reconciled societal and environmental issues in the tropics? Land Use Policy 63, 481–492.

Reed, J., van Vianen, J., Barlow, J., Sunderland, T., Sayer, J., 2020. A synthesis of evidence for achieving biodiversity, carbon, and water outcomes from forest landscape restoration. Nat. Sustain. 3, 129–137. https://doi.org/10.1038/s41893-019-0455-0.

Richardson, K., Steffen, W., Lucht, W., Bendtsen, J., Cornell, S.E., Donges, J.F., Drüke, M., Fetzer, I., Bala, G., von Bloh, W., Feulner, G., Fiedler, S., Gerten, D., Gleeson, T., Hofmann, M., Huiskamp, W., Kummu, M., Mohan, C., Nogués-Bravo, D., Petri, S., Porkka, M., Rahmstorf, S., Schaphoff, S., Thonicke, K., Tobian, A., Virkki, V., Wang-Erlandsson, L., Weber, L., Rockström, J., 2023. Earth beyond six of nine planetary boundaries. Sci. Adv. 9 (37), 1–16.

Rockstrom, J., Steffen, W., Noone, K., Persson, Å., Chapin, I.I.I., Stuart, F., Lambin, E.F., Lenton, T., Scheffer, M., Folke, C., Schellnhuber, H., Nykvist, B., de Wit, C., Hughes, T., Van der Leeuw, S., Rodhe, H., Sörlin, S., Snyder, P., Costanza, R., Svedin, U., Foley, J., 2009. A safe operating space for humanity. Nature 461, 472–475.

Sahu, R.K., Rawat, A.K., Rao, D.L.N., 2015. Traditional rainwater management system ('Haveli') in Vertisols of Central India improves carbon sequestration and biological soil fertility. Agric. Ecosyst. Environ. 200, 94–101. https://doi.org/10.1016/j.agee.2014.11.005.

Sayer, J., Sunderland, T., Ghazoul, J., Pfund, J.-L., Sheil, D., Meijaard, E., Venter, M., Boedhihartono, A.K., Day, M., Garcia, C., Garcia, C., van oosten, C., Buck, L., 2013. Ten principles for a landscape approach to reconciling agriculture, conservation, and other competing land uses. Proc. Natl. Acad. Sci. USA 110, 8349–8356.

Shakeel, A., Jamal, A., Zaidy, M.N., 2012. A regional analysis of food security in Bundelkhand region (Uttar Pradesh, India). J. Geogr. Reg. Plann. 5, 252–262. https://doi.org/10.5897/JGRP12.023.

Sharda, V.N., Kurothe, R.S., Sena, D.R., Pande, V.C., Tiwari, S.P., 2006. Estimation of groundwater recharge from water storage structures in a semi-arid climate of India. J. Hydrol. 329, 224–243.

Sharma, A., Sajjad, H., Bhuyan, N., Rahaman, M.H., Ali, R., 2024. Climate change-induced landslide vulnerability: empirical evidence from Shimla district, Himachal Pradesh, India. Int. J. Disaster Risk Reduct. 110, 104657.

Singh, P.K., Verma, S.K., Moreno, J.A., Singh, V.K., Malviya, V.P., Oliveira, E.P., Mishra, S., 2019. Geochemistry and Sm Nd isotope systematics of mafic-ultramafic rocks from the Babina and Mauranipur greenstone belts, Bundelkhand craton, India: implications for tectonic setting and Paleoarchean mantle evolution. Lithos 330, 90–107. https://doi.org/10.1016/j.lithos.2019.02.010.

Singh, R., Akuraju, V., Anantha, K.H., Garg, K.K., Barron, J., Whitbread, A.M., Dev, I., Dixit, S., 2022. Traditional rainwater management (Haveli cultivation) for building system level resilience in a fragile ecosystem of Bundelkhand region, Central India. Front. Sustain. Food Syst. 6, 826722. https://doi.org/10.3389/fsufs.2022.826722.

Singh, R., Garg, K.K., Anantha, K.H., Venkataradha, A., Dev, I., Dixit, S., Dhyani, S.K., 2021. Building resilient agricultural system through groundwater management interventions in degraded landscapes of Bundelkhand region, Central India. J. Hydrol. Reg. Stud. 37, 100929. https://doi.org/10.1016/j.ejrh.2021.100929.

Singh, R., Garg, K.K., Wani, S.P., Tewari, R.K., Dhyani, S.K., 2014. Impact of water management interventions on hydrology and ecosystem services in GarhkundarDabar watershed of Bundelkhand region, Central India. J. Hydrol. 509, 132–149. https://doi.org/10.1016/j.jhydrol.2013.11.030.

Stanturf, J.A., 2021. Landscape degradation and restoration. Soils Landsc. Restorat 125–159. https://doi.org/10.1016/b978-0-12-813193-0.00005-9.

Sun, G., Vose, J.M., McNulty, S.G., Amatya, D.M., Liang, Y., Callahan, T.J., 2018. Forest–water interactions: concepts, methodologies, and applications. J. Hydrol. 558, 159–171. https://doi.org/10.1016/j.jhydrol.2018.01.033.

van Griensven, A., Ndomba, P., Yalew, S., Kilonzo, F., 2016. Critical review of SWAT applications in Africa. Water 8, 205. https://doi.org/10.3390/w8050205.

Varua, M.E., Ward, J., Maheshwari, B., Dave, S., Kookana, R., 2018. Groundwater management and gender inequalities: the case of two watersheds in rural India. Groundw. Sustain. Dev. 6, 93–100. https://doi.org/10.1016/j.gsd.2017.11.007.

Vogt, J.V., Safriel, U., Von Maltitz, G., Sokona, Y., Hill, J., Nasi, R., Neely, C., 2021. Land restoration for achieving SDG 15.3: the role of land degradation neutrality. Environ. Sci. Pol. 123, 11–20. https://doi.org/10.1016/j.envsci.2021.05.008.

Wiebe, R.A., Wilcove, D.S., 2025. Global biodiversity loss from outsourced deforestation. Nature 639, 389–394. https://doi.org/10.1038/s41586-024-08569-5.

Xie, H., Zhang, Y., Zhai, X., Lu, C., 2020. Impacts of land degradation on ecosystem services: a review. Ecol. Indic. 111, 106435. https://doi.org/10.1016/j.ecolind.2019.106435.

Zhang, Ge, Xue, Jiacong, Liu, Wenting, Wang, Yuntao, Wang, Guoqiang, Xue, Baolin, 2025. Assessing the runoff response to vegetation cover and climate change in a typical forested headwater watershed. Water Resour. Manag. 39, 4295–4315. https://doi.org/10.1007/s11269-025-04155-0.